



Research Article

Mechanochemical Synthesis, Characterization, and Antibacterial Evaluation of Ni(II) and Cu(II) Complexes Derived from a Schiff Base Ligand

Ibrahim Waziri^{1*}, Mercy S. Ogunmodede^{1,2}, Grema A. Mala¹, Bala Isa³, Abubakar A. Ahmed¹, Hussaini B. Adam³, and Salihu A. Musa

¹Department of Pure and Applied Chemistry, University of Maiduguri, P.M.B. 1069, Maiduguri, Borno State, Nigeria

²Department of Chemistry, Faculty of Natural and Applied Sciences, Nigerian Army University, Biu, P.M.B. 1500, Biu, Borno State, Nigeria

³Department of Chemistry, Borno State University, Maiduguri, Borno state, Nigeria

*Corresponding author's Email: triumph2236@gmail.com, doi.org/10.55639/607.02010036

ARTICLE INFO: ABSTRACT

Keywords:

Metal complexes,
Schiff base,
Antimicrobial,
Mechanochemical synthesis

Metal complexes derived from Schiff bases ligands stand at the forefront of research aiming to develop precise and potent therapeutic agents, owing to their exceptional effectiveness. In this study, naphthaldehyde-derived Schiff base Ligand (HL) was synthesized *via* a mechanochemical reaction between 2-hydroxy-1-naphthaldehyde and 4-iodoaniline. Subsequently, the ligand was further reacted with Ni(II) and Cu(II) ions using their respective metal salts to obtain homoleptic mononuclear complexes (C1 and C2). The composition of HL, C1, and C2 were determined using ¹H and ¹³C NMR, UV-Vis, FTIR, CHN, and HRMS analyses. The results of these analyses revealed the ligand acted as bidentate mono-negative and chelate the metal ions through oxygen and nitrogen atoms of phenolate and azomethine moieties. Furthermore, the antibacterial potential of HL, C1, and C2 was assessed using *in vitro* disc diffusion techniques against selected bacteria, including Gram-positive *Staphylococcus aureus* and *Streptococcus pyogenes*, and Gram-negative *Escherichia coli* and *Klebsiella pneumoniae*, at concentration ranges of 10, 20, and 30 µg/mL, in comparison to the positive control (ciprofloxacin). The antibacterial study demonstrated concentration-dependent activity, with the complexes surpassing the ligand in effectiveness against all tested bacteria at all concentrations. Notably, the Cu(II) complex, C2, exhibited superior activity compared to the Ni(II) complex, C1. C2 recorded higher zone of inhibition of 30.0±0.05 mm and 28.0±0.05 mm on *S. aureus* and *E. coli*, respectively. These findings establish a robust foundation for further refining the lead compound to unlock its therapeutic potential in addressing the escalating challenge of bacterial resistance to antibiotics.

Corresponding author: Ibrahim Waziri, **Email:** triumph2236@gmail.com
Department of Pure and Applied Chemistry, University of Maiduguri, Borno State, Nigeria

INTRODUCTION

The use of metal-based complexes in medicinal chemistry has garnered significant attention due to their diverse and potent biological activities. Metal ions, with their unique coordination abilities and electronic properties, form complexes with various organic ligands that exhibit enhanced stability and, in many cases, improved biological activities (Adhikari *et al.*, 2024; Karges *et al.*, 2021; Loginova *et al.*, 2020). These metal complexes, particularly those involving transition metals, have been found to possess a wide range of pharmacological activities, including antimicrobial, anticancer, and antidiabetic properties. Transition metals such as copper, iron, cobalt, and nickel, when coordinated with appropriate ligands, have demonstrated remarkable therapeutic potential, making them important candidates for drug discovery and design (Claudel *et al.*, 2020; Frei, 2020; Shumi *et al.*, 2022).

Among the various types of ligands used to coordinate with metal ions, Schiff bases are of particular interest due to their ability to form stable, highly coordinating complexes (Boulechfar *et al.*, 2023; Felemban *et al.*, 2025). Schiff bases are typically synthesized through the condensation reaction between a primary amine and a carbonyl compound, such as an aldehyde or ketone. These ligands have a versatile coordination sphere due to the nitrogen atom in the imine group, which can bind to the metal ion, while the oxygen or other donor atoms from the ligand provide further coordination (Boulechfar *et al.*, 2023; Mushtaq *et al.*, 2024; Pathan & Patel, 2023; Dağ, 2025; Mir & Banik, 2025; Sinicropi *et al.*, 2022).

The biological potential of Schiff base-derived metal complexes has been well-documented, with numerous studies highlighting their antimicrobial, anticancer, and antifungal properties (Arun *et al.*, 2024; Chinnasamy *et al.*, 2025; Thakur *et al.*, 2024; Kanwal *et al.*, 2022; Malik *et al.*, 2018; Mezgebe & Mulugeta, 2024). Several studies have reported the antimicrobial potential of Schiff base complexes, with Ni(II) and Cu(II) complexes standing out due to their ability to interact with bacterial cell walls and disrupt cellular functions. These complexes have shown excellent antimicrobial activity, likely due to the metal ion's ability to interfere with the bacterial cell's enzymatic processes and its

ability to enhance the ligand's reactivity through metal-ligand coordination (Al-Qadsy *et al.*, 2023; El-Ghamry *et al.*, 2022; Saravanaselvam *et al.*, 2025).

Incorporating nickel into Schiff base complexes offers several advantages. Nickel and copper are biologically relevant transition metals, essential for the activity of several metalloenzymes involved in key biochemical processes. Their ability to coordinate with diverse ligands and its relatively low toxicity compared to other transition metals like iron and cobalt make them attractive candidate for drug development. Additionally, these complexes have been shown to possess significant antibacterial properties, especially against Gram-negative bacteria, which are often more resistant to conventional antibiotics. The antibacterial mechanism of Ni(II) and Cu(II) Schiff base-derived complexes is thought to involve disruption of the bacterial cell membrane, inhibition of enzymes, and interference with DNA replication processes (Chohan *et al.*, 2002; Islam *et al.*, 2025; Islam *et al.*, 2024; Yu *et al.*, 2017).

In recent years, the mechanochemical synthesis approach has gained attention as a green and sustainable method for synthesizing metal complexes and ligands. This solid-state method offers several advantages, including the absence of solvents, lower energy consumption, and reduced environmental impact. Mechanochemical synthesis is highly efficient and allows for the preparation of metal-ligand complexes in shorter reaction times, making it an attractive alternative to traditional solution-based methods (Espro & Rodriguez-Padron, 2021; Ozer, 2021; Penczner *et al.*, 2024; Reynes *et al.*, 2024). By eliminating the need for organic solvents, this approach aligns with the principles of green chemistry, making it a more sustainable option for the synthesis of metal complexes. Studies have demonstrated that mechanochemically synthesized complexes exhibit similar or even superior properties compared to those obtained through conventional methods (Brown *et al.*, 2023; Martinez *et al.*, 2023; Rabiee, 2023), showcasing their potential in the development of new materials with enhanced biological activity.

Despite the promising biological activities of Schiff base-derived metal complexes, there remains a limited understanding of their

structure–activity relationships when synthesized through green, solvent-free methods such as mechanochemistry. Furthermore, studies combining halogen-substituted aniline derivatives, like 4-iodoaniline, with bioactive aldehydes for the purpose of tuning the electronic and biological properties of Ni(II) and Cu(II) complexes are still scarce. Most existing research relies on conventional synthesis approaches and does not fully explore the potential advantages of sustainable techniques in enhancing biological efficacy. Therefore, there is a need to develop and investigate novel Schiff base-metal complexes synthesized *via* mechanochemical routes to bridge this gap and evaluate their therapeutic potential.

In the present study, we focus on the synthesis of Ni(II) and Cu(II) complex (C1 and C2) formed with a Schiff base ligand derived from 4-iodoaniline and 2-hydroxy-1-naphthaldehyde using a mechanochemical approach. The choice of 4-iodoaniline is driven by its electron-withdrawing iodine group, which is expected to influence the electronic properties of the Schiff base ligand, enhancing its ability to coordinate with the Ni(II) and Cu(II) ions. Additionally, 4-iodoaniline is known for its own biological activities, including antimicrobial properties, which may synergistically enhance the biological activity of the resulting complex (Hong *et al.*, 2000; Hu *et al.*, 2012; Kádár *et al.*, 2001). The 2-hydroxy-1-naphthaldehyde, on the other hand, contributes aromaticity and a hydroxyl group capable of coordinating with the metal ion, further stabilizing the complex. The combination of these two compounds is expected to result in a Schiff base ligand with enhanced coordination and biological properties, making it an ideal candidate for metal complexation (Cinčić & Kaitner, 2011; Das & Goswami, 2017; Martínez *et al.*, 2011; Rao *et al.*, 2003).

2.0. Experimental

2.1. Materials and Physical Measurements

The reagents and solvents used in this study were obtained from Merck Life Science (Pty) Ltd. All were of analytical grade and used without further purification. These included 4-iodoaniline, 2-hydroxy-1-naphthaldehyde, nickel(II) acetate, copper(II) acetate, and

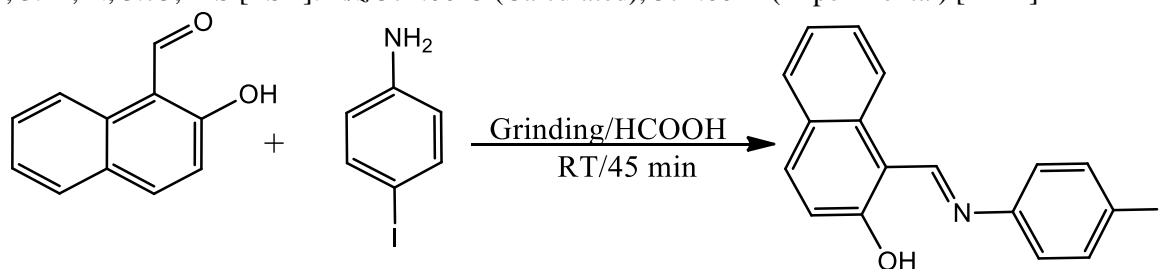
formic acid. Melting points were recorded using a MEL-TEMP electrothermal apparatus (model: 1002D) without correction. Infrared spectra were recorded using a Bruker Tensor 27 and a Perkin-Elmer FT-IR spectrometer. Elemental analysis (CHN) was performed using a VarioElementar III CHNS analyzer. Electronic spectra were obtained with a Shimadzu UV-1900 UV-Visible spectrophotometer at room temperature. NMR experiments were carried out on a Bruker 500 MHz spectrometer (500 MHz for ^1H and 125 MHz for ^{13}C), with DMSO- d_6 used for both proton and carbon analyses. Chemical shifts were reported in parts per million (ppm) relative to DMSO- d_6 , with $\delta_{\text{H}} = 2.50$ and $\delta_{\text{C}} = 39.50$ for ^1H and ^{13}C NMR spectra, respectively. Mass spectra were obtained using high-resolution mass spectrometry on a Waters Acquity UPLC Synapt G2HD machine. Thermogravimetric analysis (TGA) was conducted on a STDQ600 thermoanalyzer with a heating rate of $10^\circ\text{C}/\text{min}$ under nitrogen flow.

2.2. Synthesis

2.2.1. Synthesis of the Schiff base ligand (HL)

The Schiff base (HL) was synthesized using a modified procedure reported in the literature (Sulaiman *et al.*, 2022; Zhong & Zhong, 2014; Zhu *et al.*, 2000). To begin, 2-hydroxy-1-naphthaldehyde (0.5 g, 2.9 mmol, 1 equiv.) was weighed and placed in an agate mortar. Then, 4-iodoaniline (0.64 g, 2.9 mmol, 1 equiv.) was added, and the mixture was ground continuously at room temperature. After 20 minutes of grinding, three drops of formic acid were added as a catalyst to aid the condensation reaction and facilitate the removal of water molecules. Grinding continued for an additional 25 minutes, bringing the total reaction time to 45 minutes. This process resulted in the formation of a loose, golden powder. The product was allowed to dry in a desiccator over calcium chloride. After drying, the product was weighed, and the percentage yield was estimated using a standard procedure. It was then subjected to various characterization techniques for structural elucidation. The reaction pathway is shown in **Scheme 1**.

Golden solid; Yield: 1.01 g (93 %); m.p: 138-142 °C; ^1H NMR (500 MHz, DMSO- d_6): δ (ppm): 7.09 (t, 1H, $J_{\text{HH}} = 7.5$ Hz, Ar-H), 7.15 (d, 1H, $J_{\text{HH}} = 9.0$ Hz, Ar-H), 7.41 (t, 1H, $J_{\text{HH}} = 7.5$ Hz, Ar-H), 7.54 (t, 1H, $J_{\text{HH}} = 8.0$ Hz, Ar-H), 7.58 (t, 1H, $J_{\text{HH}} = 8.0$ Hz, Ar-H), 7.77 (d, 1H, $J_{\text{HH}} = 8.0$ Hz, Ar-H), 7.86 (d, 1H, $J_{\text{HH}} = 8.0$ Hz, Ar-H), 7.98 (d, 1H, $J_{\text{HH}} = 7.5$ Hz, Ar-H), 8.02 (d, 1H, $J_{\text{HH}} = 9.0$ Hz, Ar-H), 8.54 (d, 1H, $J_{\text{HH}} = 8.5$ Hz, Ar-H), 9.63 (s, 1H, HC=N), 15.15 (s, 1H, OH); ^{13}C NMR (125 MHz, DMSO- d_6): δ (ppm): 96.0, 109.3, 119.9, 120.4, 120.8, 124.1, 127.4, 128.4, 129.2, 130.0, 132.9, 147.9 (Ar-C), 159.0 (C-O, Ar-C), 165.5 (C=N); IR_{ATR}: (U, cm^{-1}): 3055 (O-H), 1620 (C=N), 1458 (C-H)bending, 1257 (C-N), 810 (C-I); UV-Vis (DMSO, 10^{-3}M): (λ , nm): 282 ($\pi \rightarrow \pi^*$), 340 ($n \rightarrow \pi^*$); Elemental Analysis (CHN), Calculated for $\text{C}_{17}\text{H}_{12}\text{INO}$: C, 54.71, H, 3.24, N, 3.75; Experimental for $\text{C}_{17}\text{H}_{12}\text{INO}$: C, 54.69, H, 3.24, N, 3.73; MS [ESI $^+$]: m/z 374.0045 (Calculated), 374.0042 (Experimental) $[\text{M}+\text{H}]^+$

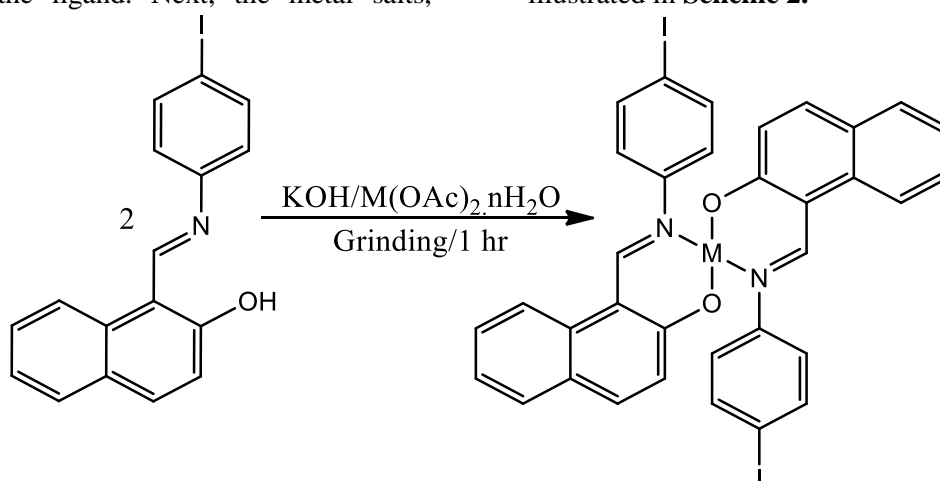


Scheme 1: Route for the synthesis of the Schiff base ligand (HL)

2.2.2. Synthesis of the complexes (C1 and C2)

The metal complexes of Ni(II) and Cu(II) (C1 and C2) with the synthesized ligand were obtained at room temperature using a modified mechanochemical method, as reported in the literature (Zhong & Zhong, 2014). To synthesize the metal complexes, 0.5 g (1.34 mmol, 2 equiv.) of the synthesized ligand (HL) was weighed and transferred into an agate mortar. KOH, 0.09 g (1.6 mmol, 2.2 equiv.) was then added to the mortar. The mixture was ground for 30 minutes until a homogeneous mixture was achieved, resulting in a darker color of the ligand. Next, the metal salts,

Ni(OAc) $_2 \cdot 4\text{H}_2\text{O}$ (0.17 g, 0.67 mmol, 1 equiv.) and Cu(OAc) $_2$ (0.12 g, 0.67 mmol, 1 equiv.), were added to the ligand-KOH mixture, and the grinding continued for an additional 30 minutes, bringing the total reaction time to 1 hour. This process resulted in light green and brown solid products for Ni(II) and Cu(II), C1 and C2, respectively. The products were then washed with ether, filtered, and dried in a desiccator over fused calcium chloride for three days. After drying, the products were weighed, and the percentage yield was estimated. The complexes were subsequently characterized. The reaction pathway is illustrated in **Scheme 2**.



Scheme 2: Route for the synthesis of the complexes (C1 and C2); M = Ni(II) or Cu(II), n = 0 or 4

Bis 1-(((4-iodophenyl)imino)methyl)naphthalen-2-olate nickel(II) (C1)

Light green solid, Yield: 0.10 g (68%); m.p.: 252-255 °C; IR_{ATR}: (U, cm⁻¹): 2967 (C-H) 1598 (C=N), 1412 (C-H)bending, 1309 (C-N), 837 (C-I); 534 (Ni-N), 451(Ni-O); UV-Vis (DMSO, 10⁻³M); (λ, nm): 265 (π→π*), 381 (n→π*), 591 (d→d); Elemental Analysis (CHN), Calculated for C₃₄H₂₂I₂N₂NiO₂: C, 50.85, H, 2.76, N, 3.49; Experimental for C₃₄H₂₂I₂N₂NiO₂: C, 50.83, H, 2.75, N, 3.46; MS [ESI⁺]: m/z 840.88 (Calculated), 840.8762 (Experimental) [M+K]⁺

Bis 1-(((4-iodophenyl)imino)methyl)naphthalen-2-olate copper(II) (C2)

Brown solid, Yield: 0.13 g (73%); m.p.: 271-273 °C; IR_{ATR}: (U, cm⁻¹): 2667 (C-H) 1583 (C=N), 1420 (C-H)bending, 1315 (C-N), 840 (C-I); 557 (Ni-N), 431(Ni-O); UV-Vis (DMSO, 10⁻³M); (λ, nm): 261 (π→π*), 379 (n→π*), 552 (d→d); Elemental Analysis (CHN), Calculated for C₃₄H₂₂CuI₂N₂O₂: C, 50.55, H, 2.74, N, 3.47; Experimental for C₃₄H₂₂CuI₂N₂O₂: C, 50.52, H, 2.70, N, 3.46; MS [ESI⁺]: m/z 829.90 (Calculated), 829.0941 (Experimental) [M+Na]⁺

2.3. Antibacterial Study

The synthesized Schiff base ligand (HL) and its Ni(II) and Cu(II) complexes (C1 and C2) were screened for antibacterial activity against selected bacteria, including Gram-positive *Staphylococcus aureus* and *Streptococcus pyogenes*, and Gram-negative *Escherichia coli* and *Klebsiella pneumoniae*, using a modified disc diffusion method. Ciprofloxacin, a standard antibiotic, was used as the positive control. The Schiff base and its metal complexes were dissolved in Dimethyl sulfoxide (DMSO) to produce three different concentrations: 30, 20, and 10 µg/mL. A disc of blotting paper was impregnated with samples and control solutions at concentrations of 30 µg/mL, 20 µg/mL, and 10 µg/mL. These discs were then placed on a plate coated with sensitivity testing agar that had been uniformly inoculated. Subsequently, the plates were incubated at 37 °C for 24 hours. The inhibition zones were observed and measured in millimeters using a transparent meter rule. The test was performed in triplicate, and the results are presented as mean ± SEM (Dinku *et al.*, 2024; Hossain *et al.*, 2022)

3.0. RESULTS AND DISCUSSION**3.1. Synthesis**

The Schiff base ligand used in synthesizing homoleptic nickel(II) and copper(II) complexes (C1 and C2) was obtained *via* a solid-state condensation synthesis (mechanochemical) approach in the presence of a catalytic amount of formic acid, as described in the scheme. The ligand was obtained in high yield (93 %) and then reacted with Ni(II) and Cu(II) ions in a 1:2 mole ratio of ligand to metal using the same mechanochemical technique, as illustrated in scheme 2. The complexes were obtained in moderate yield (68 % and 73 %).

Both the ligand and its complexes were found to be air and moisture stable, with the complexes exhibiting a higher melting point than the ligand. This difference suggests the formation of compounds with distinct chemical properties compared to the ligand, indicating the presence of metal ions in the complexes (El-Sonbati *et al.*, 2022). The ligand appeared golden in colour, while C1 complex appeared light green, and C2 complex appeared brown. The variation in physical appearance between the ligand and the complexes indicates complex formation. Moreover, the colours of the complexes are characteristic of transition metal complexes (Gopichand *et al.*, 2023). Solubility tests revealed that the ligand and complexes were soluble in DMSO, DMF, CHCl₃, and CH₃CN, while the ligand alone was soluble in methanol, ethanol, and CH₂Cl₂. The higher solubility of the complexes in highly polar solvents compared to the ligand suggests the complexes' high polarity and further confirms complexation (Hassan *et al.*, 2019).

3.2. Characterization**3.2.1. Elemental analysis**

The stoichiometric composition of the HL and its C1 and C2 complexes was determined through elemental analysis (C, H, and N). The specific percentage compositions are detailed in the spectral data provided under the synthetic procedure. The results from this analysis were found to align with the theoretical data, supporting the expected molecular weight and formula of the compounds. Notably, the complexes exhibited a composition of [ML₂], where M represents Ni(II) or Cu(II), L denotes the ligand. Following elemental analysis, the compounds underwent further characterization using UV-Vis, FTIR, MS, as well as ¹H and ¹³C NMR

techniques for the ligand. Comprehensive details of these characterizations and the corresponding results are elaborated below.

3.2.2. Nuclear magnetic resonance

^1H and ^{13}C NMR spectral studies were conducted to validate the formation of the compounds and elucidate their structures. However, due to the paramagnetic nature of the complexes, this study could not be extended to them, so other characterization techniques were pursued for their structural analysis. The spectra of the ligand were recorded using 500 MHz spectroscopy in deuterated dimethyl sulfoxide ($\text{DMSO-}d_6$) at room temperature, with solvent residual peaks at 2.50 ppm (for H) and 39.50 ppm (for C). The spectra obtained from this study are shown in Figures 1a-b. The proton spectrum (Figure 1a) displayed characteristic peaks that correspond to the protons in the compound. Notably, the signal due to the hydroxyl (OH) group proton appeared in the downfield region at 15.15 ppm. This is due to the electron-withdrawing effect of the oxygen atom in the OH group, which causes deshielding of the proton, resulting in its downfield resonance. (Bhagat *et al.*, 2013; Kaur *et al.*, 2025). Similarly, this signal appeared further downfield compared to what is typically observed in other Schiff base ligands (12.00-14.00 ppm) (Iftikhar *et al.*, 2018; Kadam *et al.*, 2018), likely due to the multiple aromatic rings in the naphthaldehyde moiety and iodine substituent.

Furthermore, the signal corresponding to the azomethine ($\text{HC}=\text{N}$) moiety was observed in the upfield region relative to the OH group at 9.63 ppm as a singlet, integrating to one proton. This is due to the weaker electron-withdrawing effect of the azomethine nitrogen atom compared to the oxygen atom of the hydroxyl group (Kadam *et al.*, 2018). However, the azomethine proton signal appeared further downfield compared to conventional Schiff base ligands, which typically appear around 8.00-9.00 ppm (Wang *et al.*, 2019). This shift is also attributed to the multiple aromatic rings in the compound,

alongside iodine substituent. The appearance of the azomethine proton signal, a key indicator of a Schiff base compound, confirms the successful isolation of the compound. Additionally, the presence of the signal due to the hydroxyl group confirms that the naphthaldehyde ring remains intact in the compound (Hutskalova & Sparr, 2024).

The successful isolation of the compound is further supported by the aromatic proton signals observed between 7.09 and 8.54 ppm. These signals were distributed among ten protons, each appearing in a different chemical environment. This matches the expected number of aromatic protons in the compound, with six protons from the naphthaldehyde ring and four from the 4-iodoaniline ring. Interestingly, the protons in the 4-iodoaniline ring were expected to appear in two distinct chemical environments as doublets, integrating to two protons each. However, the opposite was observed, with all four protons appearing in different chemical environments, each integrating to one proton. The observed splitting pattern and integration of the protons in the 4-iodoaniline aromatic ring could be due to the influence of the iodine atom, which induces coupling with the adjacent protons, resulting in additional splitting and the appearance of four distinct doublets (Pietruś *et al.*, 2021).

To complement the proton spectrum of the compound, the carbon spectrum was obtained (Figure 1b), and all the expected signals for the carbon atoms in the compound were observed. The signal due to the azomethine ($\text{HC}=\text{N}$) carbon atom appeared at 165.5 ppm, while the aromatic carbon atom connected to the oxygen atom of the hydroxyl group resonated at 159.07 ppm. The azomethine carbon signal appears more downfield due to the combined effects of the imine group ($\text{C}=\text{N}$) nitrogen and the double bond. The signals for the other aromatic carbons were observed between 96.0 and 147.9 ppm, which corroborates well with the total number of carbon atoms in the compound.

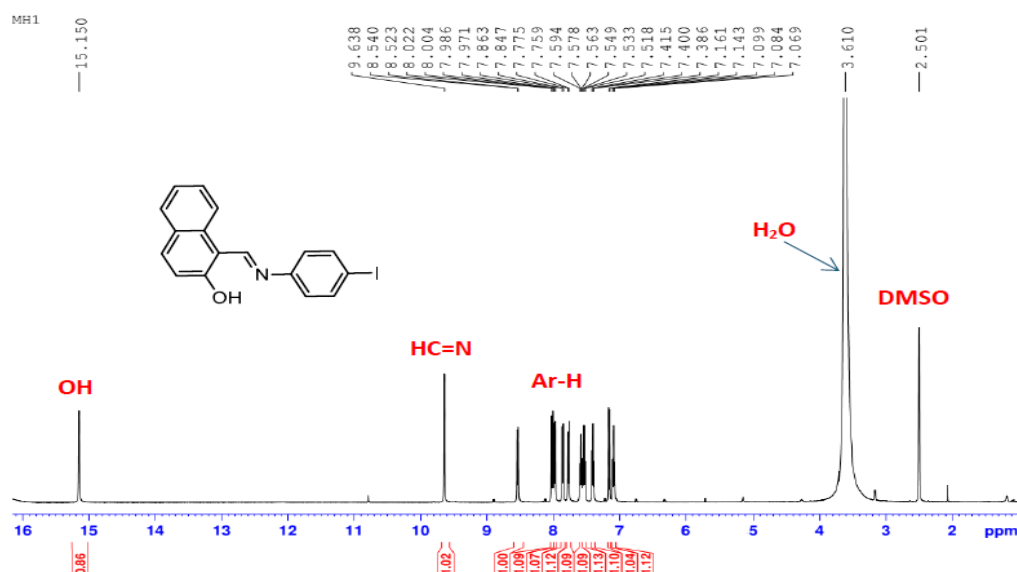


Figure 1a: ^1H NMR spectrum of the Schiff base ligand, **HL** obtained using (500 MHz, $\text{DMSO-}d_6$)

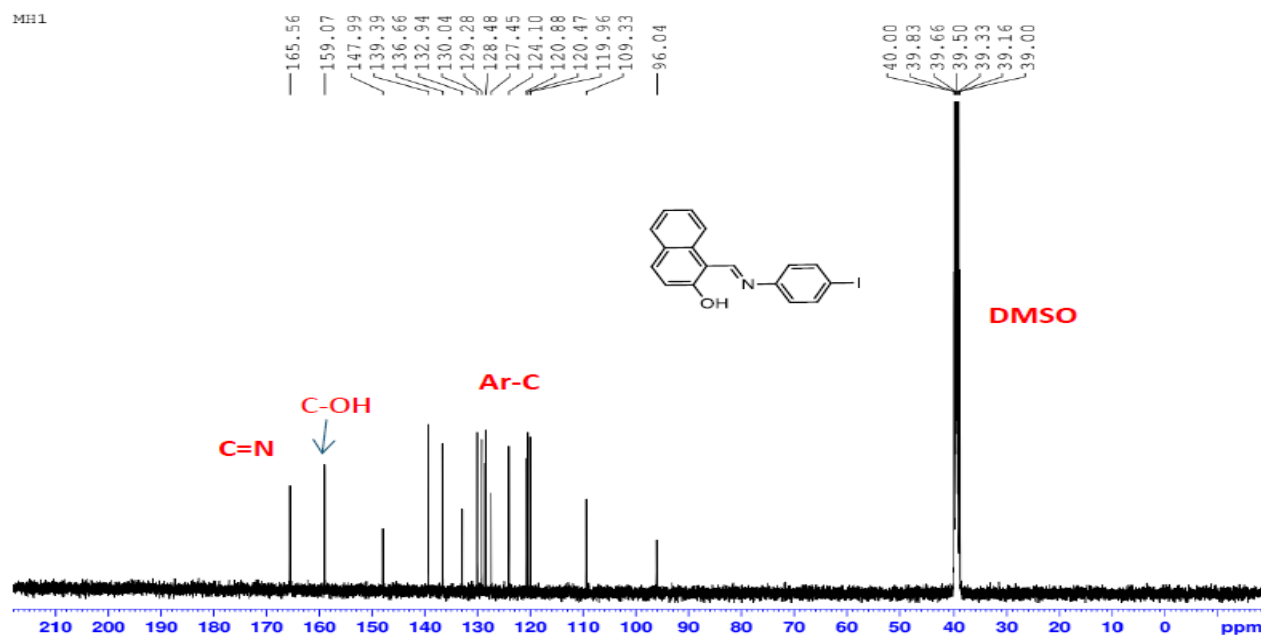


Figure 1b: ^{13}C NMR spectrum of the Schiff base ligand, **HL** obtained using (125 MHz, $\text{DMSO-}d_6$)

3.2.3. Electronic spectral study

The electronic spectra of **HL** and its complexes (**C1** and **C2**) were recorded in dimethyl sulfoxide (**DMSO**) at a concentration of 10^{-3} M. The comparative spectra are shown in Figure 2. From the spectra, the ligand (**HL**) displayed two distinct absorption bands at 263 nm and 345 nm, which are assignable to $\pi \rightarrow \pi^*$ and $n \rightarrow \pi^*$ transitions arising from the aromatic and azomethine moieties, respectively (Figure 2a). Upon complexation with Ni(II) and Cu(II) ions to form their

respective complexes (**C1** and **C2**), the spectrum of the **C1** complex shows three absorption bands at 255, 373, and 472 nm, corresponding to ($\pi \rightarrow \pi^*$), ($n \rightarrow \pi^*$), and ($d \rightarrow d$) transitions, respectively (Figure 2b). On the other hand, the spectrum of the **C2** complex displayed a similar trend with absorption at 252, 363, and 475 nm, corresponding to ($\pi \rightarrow \pi^*$), ($n \rightarrow \pi^*$), and ($d \rightarrow d$) transitions, respectively (Figure 2c) (Babu & Ayodhya, 2023; El-ghamry, Shebl, *et al.*, 2022).

Comparing the spectrum of HL with those of the metal complexes, it was noted that the band due to the ($\pi \rightarrow \pi^*$) transition shifted to a lower wavelength in the complexes (Figure 2a-c). This shift is attributed to the coordination of the metal ions to the Schiff base ligand, which alters the electronic environment and causes a blue shift. Additionally, the band due to the ($n \rightarrow \pi^*$) transition, observed at 340 nm in the free ligand, shifted to higher wavelengths at 381 and 379 nm in C1 and C2 complexes, respectively. This shift is attributed to the involvement of the azomethine nitrogen atom in coordination with the metal ions through the lone pair of electrons on the nitrogen, which reduces the electron density on the nitrogen atom and causes a red shift (Figure 2a-c) (Alorini *et al.*, 2023; El-Ghamry, Elzawawi, *et al.*, 2022).

Furthermore, both complexes exhibited additional absorption bands at 591 and 552 nm

for C1 and C2, respectively (2b-c). The absorption bands observed at 591 nm for C1 (Ni(II) complex, and 552 nm for C2 (Cu(II) complex) are assigned to d-d transitions, characteristic of Ni(II) and Cu(II) coordination complexes, respectively. These transitions are consistent with the expected electronic behaviour of octahedral (or square planar) geometries for Ni(II) and Cu(II) complexes. The presence of Schiff base ligands creates a ligand field that slightly perturbs the d-orbital energies, leading to these observed bands. Importantly, these bands are not associated with metal-to-ligand charge transfer (MLCT) transitions, which typically appear at lower wavelengths with higher intensity. This distinction supports the nature of the coordination environment around the metal centres in C1 and C2. (Devi *et al.*, 2022; Saritha & Metilda, 2021).

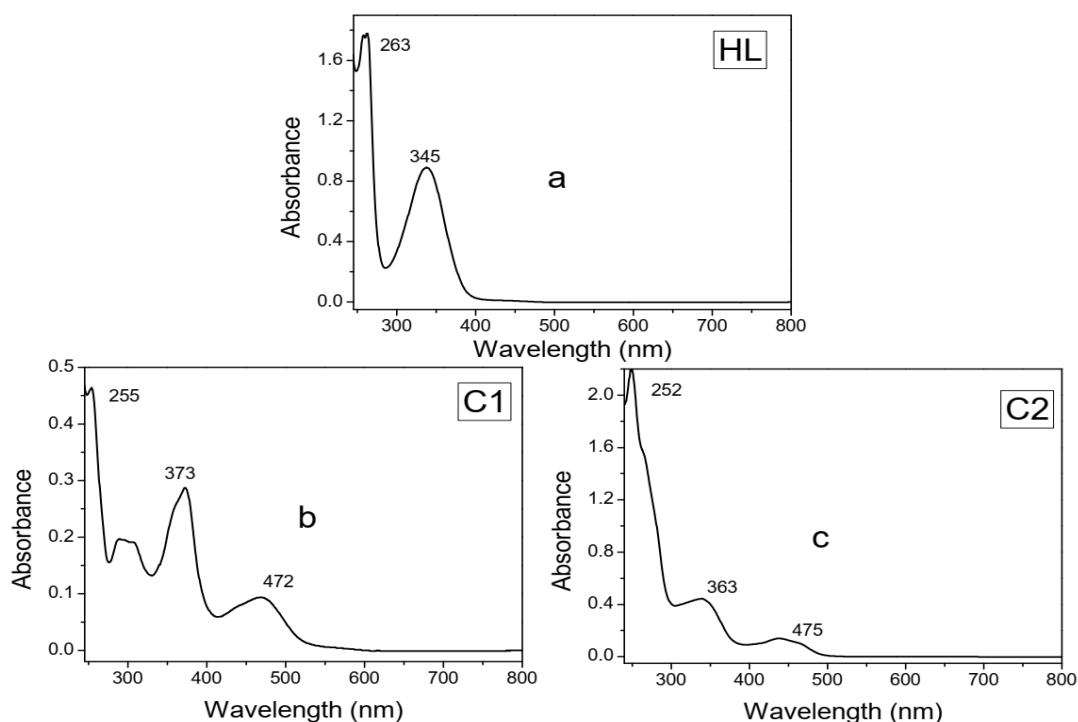


Figure 2: UV-Visible absorption spectra: (a) for the Schiff base ligand (HL), (b) for the Ni(II) complex (C1), and (c) for the Cu(II) complex (C2) obtained using 10^{-3} M sample solution in DMSO at room temperature

3.2.4. Infrared spectral study

In the IR spectrum of the free Schiff base ligand (HL) (Figure 4a), a weak absorption band for the $\nu(\text{O-H})$ bond stretching was observed at 3055 cm^{-1} (Canisares *et al.*, 2020). This band appeared weak due to the

intramolecular hydrogen bond ($\text{O-H} \cdots \text{N}$) with the azomethine nitrogen atom (Figure 3), which reduces the bond strength, making it weaker compared to the strong absorption band in compounds without intramolecular hydrogen bonding (Athokpam *et al.*, 2017).

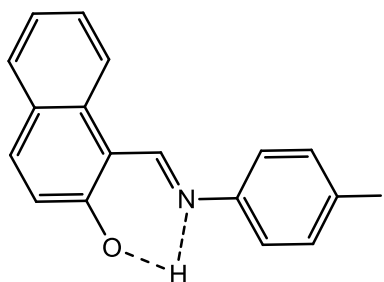


Figure 3: Illustration of the intramolecular hydrogen bond between the hydrogen atom of the hydroxyl group and the nitrogen atom of the azomethine moiety within the ligand. This bond is responsible for the appearance of the weak stretching vibration band for the hydroxyl group in the IR spectrum of HL

However, upon complexation with Ni(II) and Cu(II) ions in (C1-C2) (Figures 4b-c), this absorption band was absent in the spectra of the complexes, indicating the deprotonation of the hydroxyl group proton and the subsequent coordination of the phenolate oxygen atom to the Ni(II) and Cu(II) ions (Figures 4a-c) (Singh *et al.*, 2023). The azomethine (C=N) bond stretching frequency was observed at 1620 cm^{-1} in the spectrum of the free ligand (Figure 4a). After coordination with Ni(II) and Cu(II) ions, this stretching frequency shifted to 1598 cm^{-1} and 1583 cm^{-1} , respectively. This shift indicates the involvement of the azomethine nitrogen atom in coordination with the metal ions and the decrease in frequency due to the reduced electron density resulting from the donation of the lone electron pair to the metal ions. Similarly, the bond stretching frequencies

for other functional groups were significantly shifted upon coordination with the metal ions, reflecting the general molecular vibrations arising from coordination and the formation of new bonds (Ismaila *et al.*, 2024; Waziri *et al.*, 2023).

Furthermore, new bands were observed in the fingerprint region of the spectra of the complexes at 534 and 451 cm^{-1} for the C1 complex, and at 557 and 431 cm^{-1} for the C2 complex. These bands are attributed to M-N and M-O bond stretching vibrations (Lawan *et al.*, 2024; Waziri *et al.*, 2023) and further confirm that the ligand acts as a bidentate mono-negative ligand, coordinating to the metal centre through the nitrogen and oxygen atoms of the azomethine and phenolate moieties.

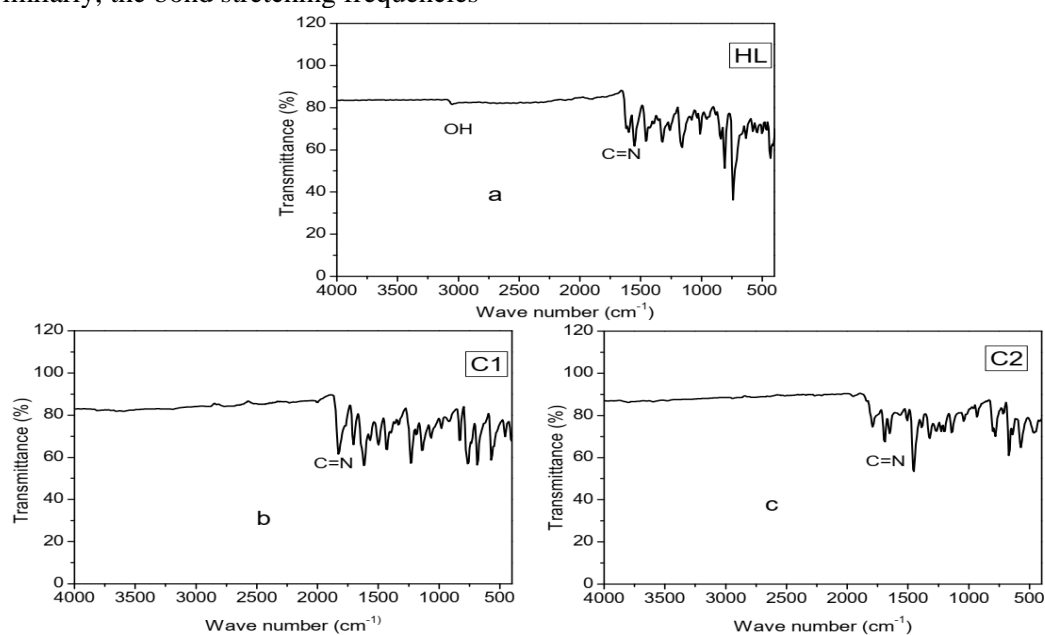


Figure 4: FTIR spectra: (a) for the Schiff base ligand (HL), (b) for the Ni(II) complex (C1), and (c) for the Cu(II) complex (C2) obtained in solid state using ATR method at room temperature.

3.2.5. Mass spectral study

Mass spectrometry is one of the most vital techniques in the structural elucidation of ligands and their complexes. This characterization method provides valuable information about molecular mass, fragmentation patterns, coordination, and isotopic patterns, which collectively contribute to determining the compound's structure and confirming the proposed structures (Ma, 2022). In this study, the mass spectra of the free ligand (HL) and its C1 and C2 complexes were obtained using high-resolution mass spectrometry after dissolving the compounds in DMSO. The spectra obtained are presented in Figures 5a-c.

The spectrum of HL (Figure 5a), obtained in $[M+H]^+$ ionization mode, shows an m/z value of 374.0045, which corresponds to the theoretical value of 374.0042. The spectrum of the C1 complex (Figure 5b), obtained in $[M+K]^+$ ionization mode, shows an m/z value of 840.8762, which corresponds to the calculated value of 840.8800. The C2 complex, obtained in $[M+Na]^+$ ionization mode, shows an m/z value of 829.0941, which corresponds to the calculated value of 829.90, (Figure 5c). The consistency between the experimental and calculated molecular weights of the compounds confirms the successful isolation of HL and its complexes (C1-C2).

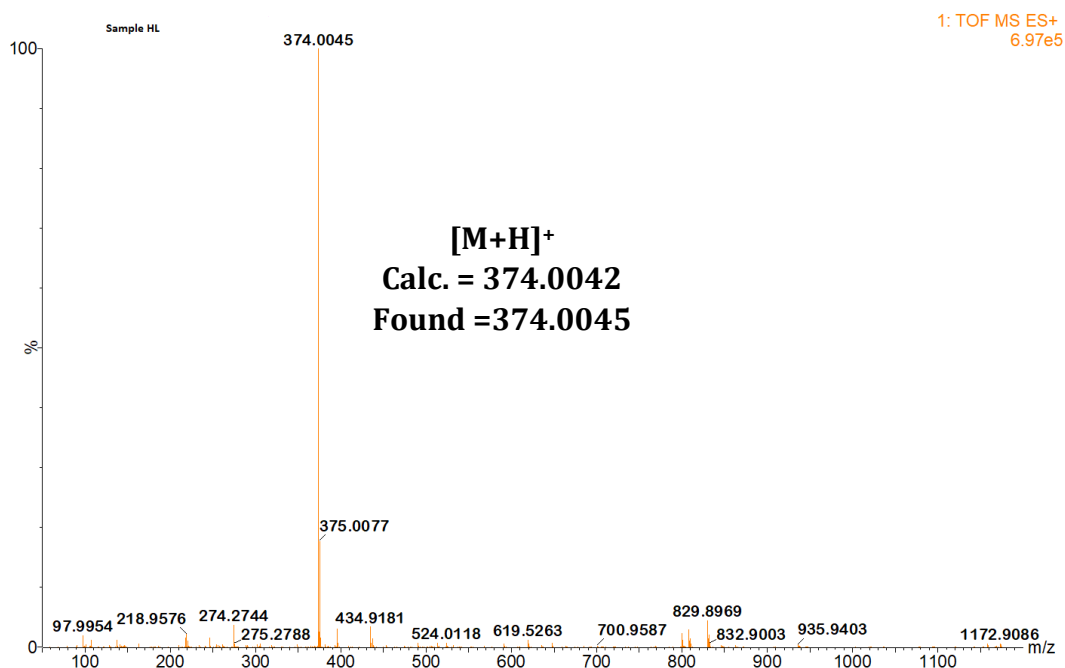


Figure 5a: Mass spectrum of **HL** obtained using a high-resolution mass spectrometer (HRMS) at room temperature, with the sample solution prepared in DMSO.

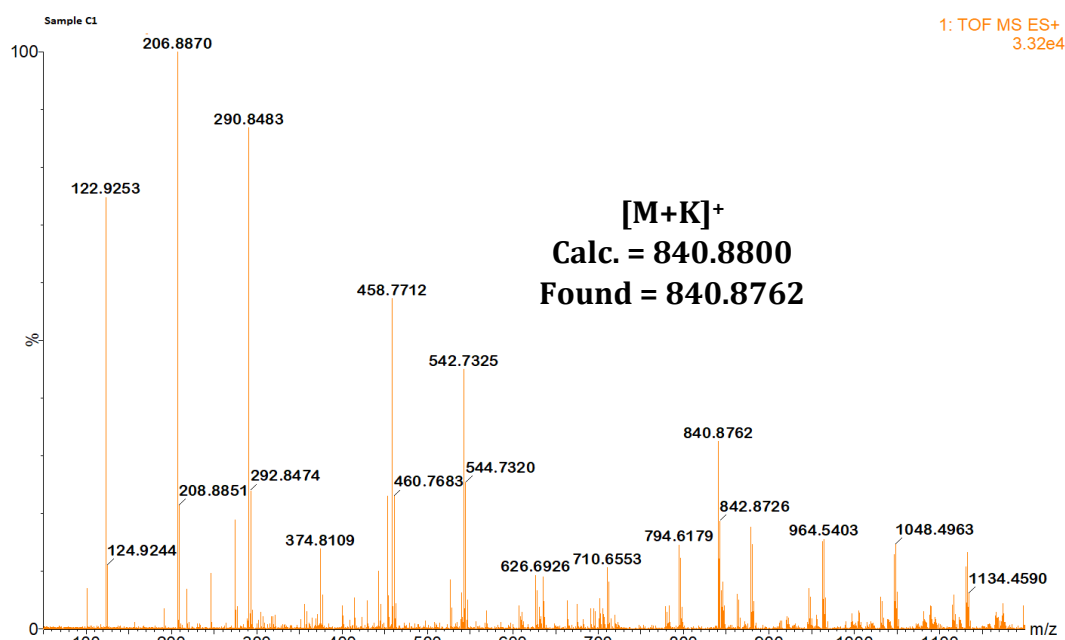


Figure 5b: Mass spectrum of **C1** obtained using a high-resolution mass spectrometer (HRMS) at room temperature, with the sample solution prepared in DMSO.

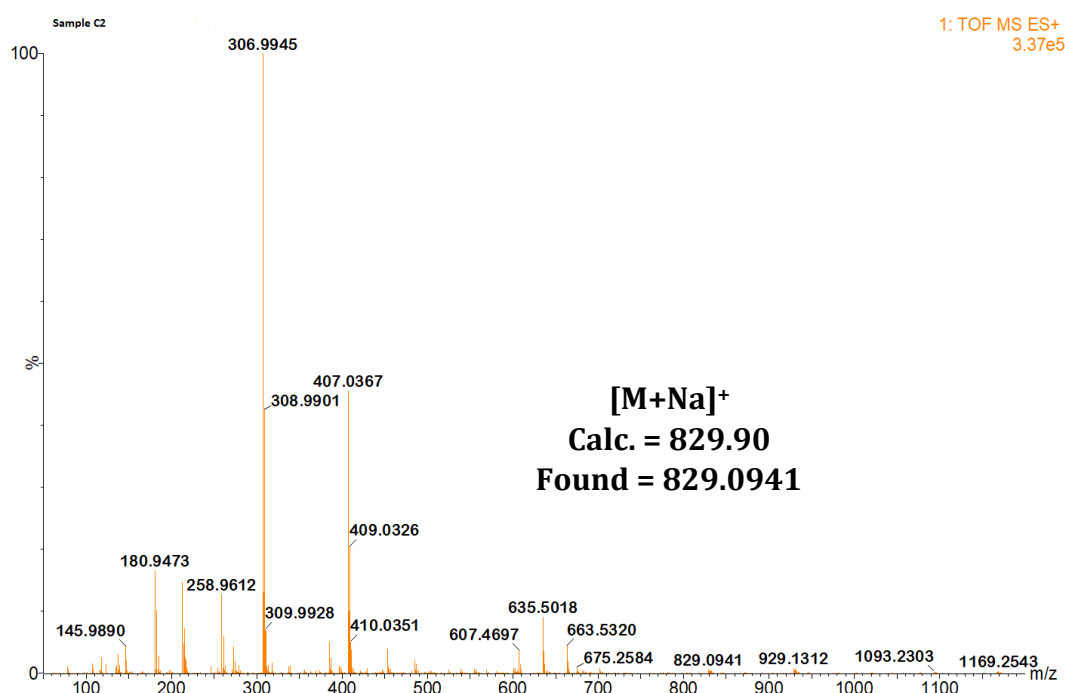


Figure 5c: Mass spectrum of **C2** obtained using a high-resolution mass spectrometer (HRMS) at room temperature, with the sample solution prepared in DMSO.

3.3. Antibacterial study

The synthesized Schiff base ligand (HL) and its Ni(II) and Cu(II) complexes (C1 and C2) were evaluated for their antibacterial activity against Gram-positive *Staphylococcus aureus* and *Streptococcus pyogenes*, as well as Gram-negative *Escherichia coli* and *Klebsiella pneumoniae*. The modified disc diffusion

method was employed at concentrations ranging from 30, 20, to 10 $\mu\text{g/mL}$. Ciprofloxacin, a standard antibiotic, served as positive control, while DMSO functioned as the negative control, being used as a solvent for compound solubilization, and details obtained are presented in Table 1.

The results of the antibacterial activity indicated that the complexes exhibited higher activity compared to the ligand at the tested concentrations, with C2 displaying superior activity than C1 and the control. Notably, DMSO, the negative control, did not show any effect on the bacteria. The activity of both the compounds and the control was found to be dependent on concentration (Table 1).

At a concentration of 10 $\mu\text{g/mL}$, the ligand HL showed no activity against any of the tested bacteria. Conversely, the Ni(II) complex C1 demonstrated zone of inhibition values of 8.0 ± 0.03 , 5.0 ± 0.2 , and 6.0 ± 0.07 mm against *S. aureus*, *S. pyogenes*, and *K. pneumoniae*, respectively, indicating inactivity against these bacteria (Table 1). At the same concentration, C2 exhibited zone of inhibition values of 12.0 ± 0.0 and 10.0 ± 0.03 mm against *S. aureus* and *E. coli*, suggesting weak activity. However, C2 showed zone of inhibition values of 8.0 ± 0.07 and 9.00 ± 0.05 mm against *S. pyogenes* and *K. pneumoniae*, respectively, indicating inactivity. Ciprofloxacin, the control, displayed weak activity against *S. aureus* and *S. pyogenes*, with zone of inhibition values of 11.0 ± 0.05 and 10.0 ± 0.04 mm, respectively. However, it demonstrated inactivity against *E. coli* and *K. pneumoniae*, with zone of inhibition values of 8.0 ± 0.01 and 6.0 ± 0.02 mm, respectively (Table 1).

As the concentration increased to 20 $\mu\text{g/mL}$, C1 exhibited zone of inhibition values of 14.0 ± 0.02 and 12.0 ± 0.04 mm against *S. aureus* and *K. pneumoniae*, indicating weak activity. At the same concentration, C2 showed moderate activity with zone of inhibition values of 18.0 ± 0.01 and 16 ± 0.01 mm against *S. aureus* and *E. coli*, respectively. It also displayed weak activity against *S. pyogenes* and *K. pneumoniae*, with zone of inhibition values of 12.0 ± 0.02 and 13.0 ± 0.08 mm, respectively (Table 1). Ciprofloxacin exhibited moderate activity against *S. aureus* and *E. coli*, with zone of inhibition values of 17.0 ± 0.04 and 15.0 ± 0.04 mm, respectively. However, it showed weak activity against *S. pyogenes* and *K. pneumoniae*, with zone of inhibition values of 13.0 ± 0.07 and 10.0 ± 0.05 mm, respectively (Table 1).

At a higher concentration of 30 $\mu\text{g/mL}$, the ligand HL displayed weak activity against *S. aureus*, *S. pyogenes*, and *K. pneumoniae*, with zone of inhibition values of 12.0 ± 0.08 , 15.0 ± 0.04 , and 11.0 ± 0.07 mm, respectively.

However, it exhibited no activity against *E. coli*, with a zone of inhibition value of 8.0 ± 0.09 mm (Table 1). For C1, at a concentration of 30 $\mu\text{g/mL}$, it demonstrated moderate activity against *S. pyogenes*, *E. coli*, and *K. pneumoniae*, with zone of inhibition values of 20.0 ± 0.03 , 17.0 ± 0.03 , and 20.0 ± 0.05 mm, respectively. Moreover, this compound showed a high level of activity against *S. aureus*, with a zone of inhibition value of 22.0 ± 0.02 mm at this concentration (Table 1). Regarding C2 at a concentration of 30 $\mu\text{g/mL}$, it exhibited higher activity against all tested bacteria, with zone of inhibition values of 30.0 ± 0.05 , 24.0 ± 0.09 , 28.0 ± 0.06 , and 25.0 ± 0.03 mm on *S. aureus*, *S. pyogenes*, *E. coli*, and *K. pneumoniae*, respectively. Similar results were observed for ciprofloxacin, with zone of inhibition values of 26.0 ± 0.03 , 25.0 ± 0.07 , 23.0 ± 0.01 , and 22.0 ± 0.03 mm on *S. aureus*, *S. pyogenes*, *E. coli*, and *K. pneumoniae*, respectively (Table 1).

The increased antibacterial activity of the complexes compared to the ligand can be attributed to factors such as the chelation effect, increased lipophilicity, altered electronic structure, and synergistic effects. As a result of this, the complexes show enhanced stability and interactions with bacterial cells, leading to improved efficacy in disrupting cellular processes. In the case of the Cu(II) complex, C2 demonstrated superior activity over the Ni(II) complex, C1, and the ligand, this can be attributed to redox activity of copper ions, favorable coordination geometry, and higher ligand affinity. The redox activity of copper ions, in particular, results in generating reactive oxygen species that are toxic to bacteria, contributing to the enhanced antibacterial properties of the C2 complex.

Table 1: Antibacterial Activity Results of the Schiff Base Ligand (HL) and Its Ni(II) and Cu(II) Complexes (C1 and C2) Obtained Using the *In vitro* Disc Diffusion Method at Various Concentrations. Zone of inhibition values are measured in millimeters (mm)^a.

Compounds	Bacteria/Concentration ($\mu\text{g}/\text{mL}$)											
	<i>S. aureus</i>			<i>S. pyogenes</i>			<i>E. coli</i>			<i>K. pneumoniae</i>		
	10	20	30	10	20	30	10	20	30	10	20	30
HL	-	-	12.0 \pm 0.08	-	-	15.0 \pm 0.04	-	-	8.0 \pm 0.09	-	-	11.0 \pm 0.07
C1	8.0 \pm 0.03	14.0 \pm 0.02	22.0 \pm 0.02	5.0 \pm 0.2	9.0 \pm 0.01	20.0 \pm 0.03	-	7.0 \pm 0.02	17.0 \pm 0.03	6.0 \pm 0.07	12.0 \pm 0.04	20.0 \pm 0.05
C2	12.0 \pm 0.07	18.0 \pm 0.01	30.0 \pm 0.05	8.0 \pm 0.02	12.0 \pm 0.02	24.0 \pm 0.03	10.0 \pm 0.03	16.0 \pm 0.01	28.0 \pm 0.06	9.0 \pm 0.05	13.0 \pm 0.08	25.0 \pm 0.03
DMSO ^c	-	-	-	-	-	-	-	-	-	-	-	-
Cipro ^b	11.0 \pm 0.05	17.0 \pm 0.04	26.0 \pm 0.03	10.0 \pm 0.04	13.0 \pm 0.07	25.0 \pm 0.03	8.0 \pm 0.01	15.0 \pm 0.04	23.0 \pm 0.01	6.0 \pm 0.02	10.0 \pm 0.05	22.0 \pm 0.03

Note: (-) = No Activity, Cipro = Ciprofloxacin, DMSO is included as a negative control due to its usage as medium for the solubilization of the compounds.

Key to interpretation: less than 10 mm = inactive, 10-15 mm = weakly active, 15-20 mm = moderately active, more than 20 mm = highly active

4.0. CONCLUSION

This study reports the synthesis of two metal complexes, Ni(II) and Cu(II) (C1 and C2), derived from the Schiff base ligand (HL). The ligand and its complexes underwent characterization using UV-Vis, FT-IR, elemental (C, H, N) analysis, mass spectroscopy, as well as ^1H and ^{13}C NMR spectroscopy. Through these analyses, it was determined that the ligand coordinated with Ni(II) and Cu(II) through the oxygen and nitrogen atoms of the phenolate and azomethine moieties, resulting in a square planar geometry around the metal ions. The *in-vitro* antibacterial study revealed that the metal complexes exhibited superior activity compared to the ligand against both gram-positive and gram-negative bacteria, with the Cu(II) complex (C2) demonstrating higher activity than the Ni(II) complex, C1, and even outperforming the positive control on some of the bacteria tested. Notably, the antibacterial activity of the compounds was found to be concentration dependent. The study has provide a platform for further optimizing the structure of the metal complexes for enhanced antimicrobial activity, and also to evaluate their toxicity profile as potential therapeutic agents. Overall, the results of this study lay a solid foundation for further research aimed at combating bacterial resistance to antibiotics and developing novel therapeutic agents.

Author contribution statement

This study was a collaborative effort among all the authors, who contributed to its conception and design. The data acquisition, analysis, and interpretation were carried out collectively. The manuscript was meticulously drafted and underwent thorough revisions by all the authors to incorporate significant intellectual content. Final approval for the publication of the manuscript was granted by all authors, indicating their unanimous agreement and endorsement of the work.

CONFLICTS OF INTEREST

The authors declare that they have no conflicts of interest regarding this study.

REFERENCES

Adhikari, S., Nath, P., Das, A., Datta, A., Baidya, N., Duttaroy, A. K., & Pathak, S. (2024). A review on metal complexes

and its anti-cancer activities: Recent updates from *in vivo* studies. *Biomedicine & Pharmacotherapy*, *171*, 116211.

- Al-Qadisy, I., Saeed, W. S., Al-Owais, A. A., Semlali, A., Alrabie, A., Al-Faqeeh, L. A. S., ALSaeedy, M., Al-Adhrai, A., Al-Odayni, A.-B., & Farooqui, M. (2023). Antimicrobial activity of novel Ni (II) and Zn (II) Complexes with (E)-2-((5-Bromothiazol-2-yl) imino) methyl phenol Ligand: Synthesis, characterization and molecular docking studies. *Antibiotics*, *12*(11), 1634.
- Arun, T. R., Kumar, H. P., & Kamalesu, S. (2024). Exploring the utilization of Schiff base metal complexes in biological settings: A review. *Inorganic Chemistry Communications*, 113251.
- Athokpam, B., Ramesh, S. G., & McKenzie, R. H. (2017). Effect of hydrogen bonding on the infrared absorption intensity of OH stretch vibrations. *Chemical Physics*, *488*, 43-54.
- Babu, K. J., & Ayodhya, D. (2023). Comprehensive investigation of Co (II), Ni (II) and Cu (II) complexes derived from a novel Schiff base: synthesis, characterization, DNA interactions, ADME profiling, molecular docking, and *in-vitro* biological evaluation. *Results in Chemistry*, *6*, 101110.
- Bhagat, S., Sharma, N., & Chundawat, T. S. (2013). Synthesis of some salicylaldehyde-based Schiff bases in aqueous media. *Journal of Chemistry*, *2013*(1), 909217.
- Boulechfar, C., Ferkous, H., Delimi, A., Djedouani, A., Kahlouche, A., Boubli, A., Darwish, A. S., Lemaoui, T., Verma, R., & Benguerba, Y. (2023). Schiff bases and their metal Complexes: A review on the history, synthesis, and applications. *Inorganic Chemistry Communications*, *150*, 110451.
- Brown, N., Alsudairy, Z., Behera, R., Akram, F., Chen, K., Smith-Petty, K., Motley, B., Williams, S., Huang, W., & Ingram, C. (2023). Green mechanochemical synthesis of imine-linked covalent organic frameworks for high iodine

- capture. *Green Chemistry*, 25(16), 6287-6296.
- Canisares, F. S., Bispo-Jr, A. G., Pires, A. M., & Lima, S. A. (2020). Syntheses and characterization of Schiff base ligands and their Ir(III) complexes as coating for phosphor-converted LEDs. *Optik*, 219, 164995.
- Chinnasamy, M., Venkatesh, N., Marimuthu, P., Sathiyam, G., Alharbi, S. A., & Venkatesan, G. (2025). Synthesis, Characterization, and Biological Evaluation of Novel Bioactive Schiff Base Metal Complexes and their Molecular Docking Studies. *Journal of Environmental Chemical Engineering*, 115835.
- Chohan, Z. H., Rauf, A., Noreen, S., Scozzafava, A., & Supuran, C. T. (2002). Antibacterial cobalt (II), nickel (II) and zinc (II) complexes of nicotinic acid-derived Schiff-bases. *Journal of enzyme inhibition and medicinal chemistry*, 17(2), 101-106.
- Cinčić, D., & Kaitner, B. (2011). Schiff base derived from 2-hydroxy-1-naphthaldehyde and liquid-assisted mechanochemical synthesis of its isostructural Cu (II) and Co (II) complexes. *crystengcomm*, 13(13), 4351-4357.
- Claudel, M., Schwarte, J. V., & Fromm, K. M. (2020). New antimicrobial strategies based on metal complexes. *Chemistry*, 2(4), 849-899.
- Dağ, A. K. (2025). New Schiff base ligands and their homoleptic Co (II)/Cu (II) complexes: synthesis, characterization and photocatalytic properties for degradation of methylene blue. *Journal of Molecular Structure*, 1327, 141185.
- Das, A. K., & Goswami, S. (2017). 2-Hydroxy-1-naphthaldehyde: A versatile building block for the development of sensors in supramolecular chemistry and molecular recognition. *Sensors and Actuators B: Chemical*, 245, 1062-1125.
- Devi, J., Kumar, S., Kumar, D., Jindal, D. K., & Poornachandra, Y. (2022). Synthesis, characterization, in vitro antimicrobial and cytotoxic evaluation of Co (II), Ni (II), Cu (II) and Zn (II) complexes derived from bidentate hydrazones. *Research on Chemical Intermediates*, 1-33.
- Dinku, D., Demissie, T. B., Beas, I. N., Eswaramoorthy, R., Abdi, B., & Desalegn, T. (2024). Antimicrobial activities and docking studies of new Schiff base ligand and its Cu (II), Zn (II) and Ni (II) Complexes: Synthesis and Characterization. *Inorganic Chemistry Communications*, 160, 111903.
- El-Ghamry, M. A., Elzawawi, F. M., Aziz, A. A. A., Nassir, K. M., & Abu-El-Wafa, S. M. (2022). New Schiff base ligand and its novel Cr (III), Mn (II), Co (II), Ni (II), Cu (II), Zn (II) complexes: Spectral investigation, biological applications, and semiconducting properties. *Scientific Reports*, 12(1), 17942.
- El-Sonbati, A., El-Mogazy, M., Nozha, S., Diab, M., Abou-Dobara, M., Eldesoky, A., & Morgan, S. M. (2022). Mixed ligand transition metal (II) complexes: Characterization, spectral, electrochemical studies, molecular docking and bacteriological application. *Journal of Molecular Structure*, 1248, 131498.
- Espro, C., & Rodriguez-Padron, D. (2021). Rethinking organic synthesis: Mechanochemistry as a greener approach. *Current Opinion in Green and Sustainable Chemistry*, 30, 100478.
- Felemban, M. F., Tayeb, F. J., Alqarni, A., Ashour, A. A., & Shafie, A. (2025). Recent Advances in Schiff Base Coinage Metal Complexes as Anticancer Agents: A Comprehensive Review (2021–2025). *Dyes and Pigments*, 112710.
- Frei, A. (2020). Metal complexes, an untapped source of antibiotic potential? *Antibiotics*, 9(2), 90.
- Gopichand, K., Mahipal, V., Rao, N. N., Ganai, A. M., & Rao, P. V. (2023). Co (II), Ni (II), Cu (II), and Zn (II) complexes with Benzothiazole Schiff base ligand: Preparation, Spectral Characterization, DNA Binding, and In Vitro Cytotoxic

- Activities. *Results in Chemistry*, 5, 100868.
- Hassan, S., Adam, F., Bakar, M. A., & Mudalip, S. A. (2019). Evaluation of solvents' effect on solubility, intermolecular interaction energies and habit of ascorbic acid crystals. *Journal of Saudi Chemical Society*, 23(2), 239-248.
- Hong, S. K., Anestis, D. K., Henderson, T. T., & Rankin, G. O. (2000). Haloaniline-induced in vitro nephrotoxicity: Effects of 4-haloanilines and 3, 5-dihaloanilines. *Toxicology letters*, 114(1-3), 125-133.
- Alorini, T., Daoud, I., Al-Hakimi, A. N., & Alminderej, F. (2023). Synthesis, characterization, anticancer activity, and molecular docking study of some metal complexes with a new Schiff base ligand. *Journal of Molecular Structure*, 1276, 134785.
- Hossain, M., Khushy, K., Latif, M., Hossen, M. F., Asraf, M. A., Kudrat-E-Zahan, M., & Abdou, A. (2022). Co (II), Ni (II), and Cu (II) complexes containing isatin-based Schiff Base ligand: synthesis, physicochemical characterization, DFT calculations, antibacterial Activity, and molecular docking analysis. *Russian Journal of General Chemistry*, 92(12), 2723-2733.
- Hu, Q., Moran, J., & Gan, J. (2012). Sorption, degradation, and transport of methyl iodide and other iodine species in geologic media. *Applied geochemistry*, 27(3), 774-781.
- Hutskalova, V., & Sparr, C. (2024). Aromatic ring-opening metathesis. *Nature*, 1-2.
- Iftikhar, B., Javed, K., Khan, M. S. U., Akhter, Z., Mirza, B., & Mckee, V. (2018). Synthesis, characterization and biological assay of Salicylaldehyde Schiff base Cu (II) complexes and their precursors. *Journal of Molecular Structure*, 1155, 337-348.
- Ismaila, M. B., Mala, G. A., Umaru, U., El-Maksoud, M. S. A., Wakil, I. M., Coetzee, L. C. C., & Waziri, I. (2024). Synthesis, Characterization, Biological Evaluation, DFT, and Molecular Docking Study of a Co (II) Complex Derived from ON Donor Bidentate Schiff Base Ligand. *ChemistrySelect*, 9(40), e202403591.
- Kadam, M. M., Patil, D., & Sekar, N. (2018). 4-(Diethylamino) salicylaldehyde based fluorescent Salen ligand with red-shifted emission—A facile synthesis and DFT investigation. *Journal of Luminescence*, 204, 354-367.
- Kádár, M., Nagy, Z., Karancsi, T., & Farsang, G. (2001). The electrochemical oxidation of 4-bromoaniline, 2, 4-dibromoaniline, 2, 4, 6-tribromoaniline and 4-iodoaniline in acetonitrile solution. *Electrochimica acta*, 46(22), 3405-3414.
- Kanwal, A., Parveen, B., Ashraf, R., Haider, N., & Ali, K. G. (2022). A review on synthesis and applications of some selected Schiff bases with their transition metal complexes. *Journal of Coordination Chemistry*, 75(19-24), 2533-2556.
- Karges, J., Stokes, R. W., & Cohen, S. M. (2021). Metal complexes for therapeutic applications. *Trends in chemistry*, 3(7), 523-534.
- Kaur, S., Kaur, J., Rana, M., Sharma, J., & Kaur, I. (2025). Salicylaldehyde based Schiff base: synthesis, characterisation and application for selective electrochemical detection of Cu²⁺ in real samples. *International Journal of Environmental Analytical Chemistry*, 105(1), 20-32.
- Lawan, S. Y., Mshelia, M. B., Mala, G. A., Olaide, W. O., Musa, S. A., Ahmed, A. A., Yesufu, H. B., & Waziri, I. (2024). Antioxidant Activity and DFT Calculations of Metal Complexes Derived from a Schiff Base Ligand: Synthesis, Characterization, and Biological Evaluation. *ChemistrySelect*, 9(13), e202400676.
- Loginova, N. V., Harbatsevich, H. I., Osipovich, N. P., Ksendzova, G. A., Koval'chuk, T. V., & Polozov, G. I. (2020). Metal complexes as promising agents for biomedical applications. *Current Medicinal Chemistry*, 27(31), 5213-5249.
- Ma, X. (2022). Recent advances in mass spectrometry-based structural

- elucidation techniques. *Molecules*, 27(19), 6466.
- Malik, M. A., Dar, O. A., Gull, P., Wani, M. Y., & Hashmi, A. A. (2018). Heterocyclic Schiff base transition metal complexes in antimicrobial and anticancer chemotherapy. *MedChemComm*, 9(3), 409-436.
- Martínez, R. F., Ávalos, M., Babiano, R., Cintas, P., Jiménez, J. L., Light, M. E., & Palacios, J. C. (2011). Tautomerism in Schiff bases. The cases of 2-hydroxy-1-naphthaldehyde and 1-hydroxy-2-naphthaldehyde investigated in solution and the solid state. *Organic & Biomolecular Chemistry*, 9(24), 8268-8275.
- Martinez, V., Stolar, T., Karadeniz, B., Brekalo, I., & Užarević, K. (2023). Advancing mechanochemical synthesis by combining milling with different energy sources. *Nature Reviews Chemistry*, 7(1), 51-65.
- Mezgebe, K., & Mulugeta, E. (2024). Synthesis and pharmacological activities of Schiff bases with some transition metal complexes: A review. *Medicinal Chemistry Research*, 33(3), 439-463.
- Mir, M. A., & Banik, B. K. (2025). Synthesis of Schiff base ligands under environment friendly conditions: A systematic review. *Inorganic Chemistry Communications*, 113987.
- Mushtaq, I., Ahmad, M., Saleem, M., & Ahmed, A. (2024). Pharmaceutical significance of Schiff bases: an overview. *Future Journal of Pharmaceutical Sciences*, 10(1), 16.
- Ozer, D. (2021). Mechanochemistry: A power tool for green synthesis. In *Advances in Green Synthesis: Avenues and Sustainability* (pp. 23-39). Springer.
- Pathan, I. R., & Patel, M. K. (2023). A comprehensive review on the synthesis and applications of Schiff base ligand and metal complexes: A comparative study of conventional heating, microwave heating, and sonochemical methods. *Inorganic Chemistry Communications*, 158, 111464.
- Penczner, S. H., Kumar, P., Patel, M., Bouchard, L.-S., Iacopino, D., & Patel, R. (2024). Innovations in mechanochemical synthesis: Luminescent materials and their applications. *Materials Today Chemistry*, 39, 102177.
- Pietruś, W., Kurczab, R., Kalinowska-Tłuścik, J., Machalska, E., Golonka, D., Barańska, M., & Bojarski, A. J. (2021). Influence of Fluorine Substitution on Nonbonding Interactions in Selected Para-Halogeno Anilines. *ChemPhysChem*, 22(20), 2115-2127.
- Rabiee, N. (2023). Sustainable metal-organic frameworks (MOFs) for drug delivery systems. *Materials Today Communications*, 35, 106244.
- Rao, P. V., Rao, C. P., Wegelius, E. K., & Rissanen, K. (2003). 2-hydroxy-1-naphthaldehyde-derived Schiff bases: synthesis, characterization, and structure. *Journal of chemical crystallography*, 33, 139-147.
- Reynes, J. F., Leon, F., & García, F. (2024). Mechanochemistry for Organic and Inorganic Synthesis. *ACS Organic & Inorganic Au*, 4(5), 432-470.
- Saritha, T., & Metilda, P. (2021). Synthesis, spectroscopic characterization and biological applications of some novel Schiff base transition metal (II) complexes derived from curcumin moiety. *Journal of Saudi Chemical Society*, 25(6), 101245.
- Saravanaselvam, S. V., Arulanantham, X., Tamilelakkiya, M., Sakthivadivel, R., Ponnusamy, S., Pandi, P., Velusamy, P., Muthu, S. E., & Kumar, K. A. (2025). Synthesis and characterization of novel Schiff base ligand and their Cu (II), Zn (II), Co (II), and Ni (II) complexes: DNA binding, antimicrobial activity and docking studies. *Journal of Molecular Structure*, 1325, 141000.
- Shumi, G., Desalegn, T., Demissie, T. B., Ramachandran, V. P., & Eswaramoorthy, R. (2022). Metal Complexes in Target-Specific Anticancer Therapy: Recent Trends and Challenges. *Journal of Chemistry*, 2022(1), 9261683.

- Singh, A., Prasad, L. B., Shiv, K., Kumar, R., & Garai, S. (2023). Synthesis, characterization, and in vitro antibacterial and cytotoxic study of Co (II), Ni (II), Cu (II), and Zn (II) complexes of N-(4-methoxybenzyl) N-(phenylethyl) dithiocarbamate ligand. *Journal of Molecular Structure*, 1288, 135835.
- Sinicropi, M. S., Ceramella, J., Iacopetta, D., Catalano, A., Mariconda, A., Rosano, C., Saturnino, C., El-Kashef, H., & Longo, P. (2022). Metal complexes with Schiff bases: Data collection and recent studies on biological activities. *International Journal of Molecular Sciences*, 23(23), 14840.
- Sulaiman, Z., Na'aliya, J., & Usman, B. (2022). Mechanochemical Synthesis, Characterization and In-vitro Anti-Microbial Studies of Binuclear Cu (II) and Zn (II) Complexes with Schiff Base Derived from Phenylalanine and Vanillin. *ChemSearch Journal*, 13(1), 9–22–29–22.
- Thakur, S., Jaryal, A., & Bhalla, A. (2024). Recent advances in biological and medicinal profile of Schiff bases and their metal complexes: an updated version (2018–2023). *Results Chem* 7: 101350. In.
- Wang, Y.-A., Liu, T., & Zhong, G.-Q. (2019). Synthesis, characterization and applications of copper (II) complexes with Schiff bases derived from chitooligosaccharide and iodosubstituted salicylaldehyde. *Carbohydrate Polymers*, 224, 115151.
- Waziri, I., Lawan, S. Y., Ndahi, N. P., Galadima, I. B., Wahab, O. O., Yusuf, T. L., Coetzee, L.-C. C., & Abd El-Maksoud, M. S. Synthesis, Characterization, Anti-nematocidal, and Computational Study of Copper (II) Complex Derived from Fluoro-substituted Schiff base Ligand. *Chemistry & Biodiversity*, e202403033.
- Waziri, I., Masena, H. M., Yusuf, T. L., Coetzee, L.-C. C., Adeyinka, A. S., & Muller, A. J. (2023). Synthesis, characterization, biological evaluation, DFT and molecular docking studies of (Z)-2-((2-bromo-4-chlorophenyl) imino) methyl)-4-chlorophenol and its Co (ii), ni (ii), Cu (ii), and zn (ii) complexes. *New Journal of Chemistry*, 47(38), 17853-17870.
- Yu, H., Zhang, W., Yu, Q., Huang, F.-P., Bian, H.-D., & Liang, H. (2017). Ni (II) complexes with Schiff base ligands: preparation, characterization, DNA/protein interaction and cytotoxicity studies. *Molecules*, 22(10), 1772.
- Zhong, G.-Q., & Zhong, Q. (2014). Solid–solid synthesis, characterization, thermal decomposition and antibacterial activities of zinc (II) and nickel (II) complexes of glycine–vanillin Schiff base ligand. *Green Chemistry Letters and Reviews*, 7(3), 236-242.
- Zhu, X., Wang, C., Dang, Y., Zhou, H., Wu, Z., Liu, Z., Ye, D., & Zhou, Q. (2000). The Schiff base N-salicylidene-O, S-dimethylthiophosphorylimine and its metal complexes: synthesis, characterization and insecticidal activity studies. *Synthesis and Reactivity in Inorganic and Metal-Organic Chemistry*, 30(4), 625-636.